Spectrum-Efficient Distributed Collaborative Beamforming in the Presence of Local Scattering and Interference

Slim Zaidi and Sofiene Affes
INRS-EMT, Université du Québec, Montreal, QC, H5A 1K6, Canada,
Email: zaidi,affes@emt.inrs.ca

***Abstract*—In this paper, a minimum variance distortionless response (MVDR) collaborative beamformer (CB) is considered to achieve a dual-hop communication from a far-field source surrounded by several interfering transmitters to a receiver, through a wireless network comprised of K independent terminals. Whereas the previous works assumed a model of plane wavefronts, here, a local scattering in the source and interferences vicinities is considered, thereby broadening the range of applications in real-world environments. It is shown that the required bandwidth allocation to the MVDR CB implementation linearly increases with K and becomes prohibitive in some applications where the number of terminals is typically large. Aiming to improve the system's spectrum efficiency, a novel distributed collaborative beamformer (DCB) whose implementation does not require any bandwidth allocation and, further, that well-approximates its MVDR CB counterpart is then proposed. The performance of the proposed technique is analyzed and its net advantages against the scattering-free DCB technique, which is designed without taking into account the presence of local scattering in the source and interferences vicinities, are proved.**

***Index Terms*—distributed collaborative beamforming, local scattering, spectrum efficiency, device-to-device (D2D) communications, wireless sensor networks (WSN).**

I. Introduction

The implementation of the collaborative beamforming (CB) technique can increase the transmission coverage, the link reliability, and the capacity of wireless networks [1]-[8]. Using this technique, a set of K independent terminals (mobile users, soldiers in battlefield, sensor nodes, relays, etc) play a central role in the signal transmission flow. Indeed, these terminals or devices multiply their received signals, sent from a source and interferences, with the complex conjugates of properly selected beamforming weights, and forward the resulting signals to the receiver. In order to compute their corresponding weights, the terminals often need to exchange information with one another. This process requires a large amount of bandwidth allocation, thereby decreasing the system's spectrum efficiency. This impediment has motivated growing research efforts in designing distributed collaborative beamforming (DCB) techniques that aim to improve the system's spectrum efficiency by reducing the bandwidth allocation required to their implementations [7], [8].

Work supported by a Canada Research Chair in Wireless Communications and the Discovery Grants Program of NSERC.

In spite of their significant contributions, all the previous works neglect the effect of scattering and reflection and assume a simple model of plane wavefronts. Unfortunately, in practice, the propagation environments are often more complicated than this model. In fact, when a transmitter (source or interference) is scattered by a large number of scatterers within its vicinity, as in urban and suburban environments, several replicas of the transmit signal are generated [9]-[13]. In such a case, the signal can be modeled as a superposition of independent and identically distributed (i.i.d.) rays [9]. Commonly known as local scattering, the effect of this phenomenon on the CB technique was investigated in [10]. It has been shown that the performance of CB techniques, designed without taking into account the presence of local scattering, are deteriorated especially in urban environments wherein local scattering is relatively important. Recently, the authors of [13] have proposed a DCB technique whose design takes into account the local scattering phenomenon. Although it enhances DCB performances, the proposed approach did not consider the presence of interference. The aim of this work is then to go another significant step forward pushing the frontier of the CB applicability in real-world environments where the local scattering phenomenon and interference co-exist.

In this paper, we consider a minimum variance distortionless response (MVDR) CB to achieve a dual-hop communication from a far-field source surrounded by several interfering transmitters to a receiver, through a wireless network comprised of K independent terminals. Each transmitter (source or interference) is assumed to be scattered by a large number of scatterers within its vicinity to generate L i.i.d rays from the transmit signal. Taking into account this phenomenon, the beamforming vector is derived. Unfortunately, it turns out that terminals need to exchange information with one another to compute their corresponding weights. This process requires a large bandwidth allocation, thereby decreasing the system's spectrum efficiency. A novel DCB technique whose implementation does not require any bandwidth allocation and, further, that well-approximates its MVDR CB counterpart is then pro-

978-1-4673-0921-9/12/$31.00 ©2012 IEEE

posed. The performance of the proposed technique and its net advantages against the scattering-free DCB technique, which is designed without taking into account the presence of local scattering in the source and interferences vicinities, are verified. It is proved that the proposed technique is much more robust against local scattering than its so-called scattering-free vis-a-vis.

The rest of this paper is organized as follows. The system model is described in Section II. The beamforming vector of the MVDR CB is derived in Section III. A novel DCB technique with improved spectrum efficiency is proposed in Section IV. Section V analyzes the performance of the proposed technique while Section VI provides computer simulations. Concluding remarks are given in Section VII.

Notation: Uppercase and lowercase bold letters denote matrices and vectors, respectively. $[\cdot]_{il}$ and $[\cdot]_i$ are the (i,l)-th entry of a matrix and i-th entry of a vector, respectively. $\mathbf{I}$ is the identity matrix. $(\cdot)^T$ and $(\cdot)^H$ denote the transpose and the Hermitian transpose, respectively. $\|\cdot\|$ is the 2-norm of a vector and $|\cdot|$ is the absolute value. $\mathrm{E}\{\cdot\}$ stands for the statistical expectation and $(\xrightarrow{ep1})$ $\xrightarrow{p1}$ denotes (element-wise) convergence with probability one. $J_1(\cdot)$ is the first-order Bessel function of the first kind and $\odot$ is the element-wise product.

II. System model

As illustrated in Fig. 1, the system of our concern consists of a wireless network comprised of K uniformly distributed terminals on $D(O,R)$, the disc with center at O and radius R, a receiver at O, and M far-field transmitters including one source and the rest act as interferences. We assume that there is no direct link from the transmitters to the receiver. Moreover, let (r_k,ψ_k) denote the polar coordinates of the k-th node and (A_m,ϕ_m) denote those of the m-th transmitter where (A_1,ϕ_1) is assumed to be the location of the source with $\phi_1=0$. It also assumed that $A_m \gg R$ for $m=1,\ldots,M$. The following assumptions

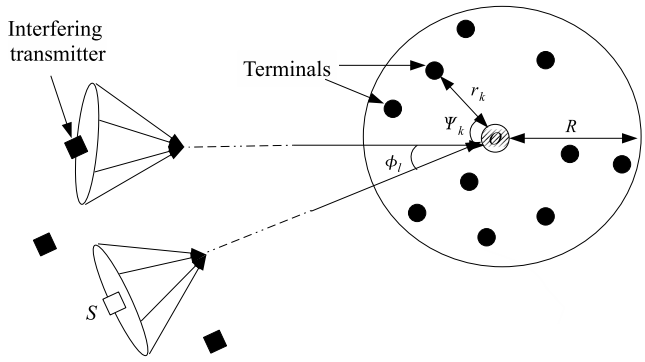

Fig. 1. System model.

are further made:

A1) Each transmitter is scattered by a large number of scatterers within its vicinity to generate L equal-power rays. The l-th ray is characterized by its direction θ_l and its complex amplitude $\alpha_l=\rho_l e^{j\xi_l}$ where the amplitudes $\rho_l,\ l=1,\ldots,L$ and the phases $\xi_l,\ l=1,\ldots,L$ are i.i.d. random variables, and each phase is uniformly distributed over $[-\pi,\pi]$. The $\theta_l,\ l=1,\ldots,L$ are also i.i.d. random variables distributed with variance σ_θ^2 and probability density functions (pdf) $p(\theta)$ [9]-[13]. All θ_ls, ξ_ls, and ρ_ls are mutually independent.

A2) The channel gain $[\mathbf{f}]_k$ from the k-th terminal to the receiver is a zero-mean unit-variance circular Gaussian random variable.

A3) The m-th transmitter's signal s_m is a zero-mean random variable with power p_m while noises at terminals and the receiver are zero-mean Gaussian random variables with variances ${\sigma_v}^2$ and ${\sigma_n}^2$, respectively. All signals, noises, and the terminals' forward channel gains are mutually independent.

A4) The k-th terminal is aware of its own coordinates (r_k,ψ_k), its forward channel $[\mathbf{f}]_k$, the directions of the transmitters $\phi_m,\ m=1,\ldots,M$, σ_v^2, K, and σ_θ, while being oblivious to the locations and the forward channels of *all* other terminals in the network.

Using A1 and the fact that $A_m \gg R$ for $m=1,\ldots,M$, the channel gain from the m-th transmitter to the k-th terminal can be represented as

$$[\mathbf{g}_m]_k=\sum_{l=1}^{L}\alpha_l e^{-j\frac{2\pi}{\lambda}r_k\cos(\phi_m+\theta_l-\psi_k)} \tag{1}$$

where λ is the wavelength.

III. MVDR CB in the presence of local scattering

A dual-hop communication is established from the M transmitters to the receiver. In the first time slot, all transmitters send their signals to the wireless network. Let $\mathbf{y}$ denote the received signal vector at terminals given by

$$\mathbf{y}=\mathbf{G}\mathbf{s}+\mathbf{v} \tag{2}$$

where $\mathbf{s}\triangleq[s_1 s_2\ldots s_m]^T$, $\mathbf{G}\triangleq[\mathbf{g}_1\ldots\mathbf{g}_M]$, and $\mathbf{v}$ is the terminals' noise vector. In the second time slot, the k-th terminal multiplies its received signal with the complex conjugate of the beamforming weight w_k and forwards the resulting signal to the receiver. The terminals transmitted signal vector can then be represented as

$$\mathbf{x}=\mathbf{w}^*\odot\mathbf{y} \tag{3}$$

where $\mathbf{w}\triangleq[w_1\ldots w_K]$ is the beamforming vector. It follows from (2) and (3) that the received signal at O is

$$r=s_1\mathbf{w}^H\mathbf{h}_1+\mathbf{w}^H\mathbf{H}_{\bar{1}}\mathbf{s}_{\bar{1}}+\mathbf{w}^H(\mathbf{f}\odot\mathbf{v})+n \tag{4}$$

where n is the receiver noise, $\mathbf{s}_{\bar{1}}\triangleq[s_2\ldots s_M]^T$, $\mathbf{h}_1\triangleq\mathbf{f}\odot\mathbf{g}_1$ and $\mathbf{H}_{\bar{1}}\triangleq[\mathbf{f}\odot\mathbf{g}_2\ldots\mathbf{f}\odot\mathbf{g}_M]$ with $\mathbf{f}\triangleq[[\mathbf{f}]_1\ldots[\mathbf{f}]_K]^T$.

Let P^{S}, P^{I}, and P^{N} denote the received power from the source, the received power from the interferences, and the aggregate noise power due to the thermal noise at

the receiver and the forwarded noises from the terminals, respectively. It holds from (4) that

$$P_{\mathbf{w}}^{\mathrm{S}} = p_1 \mathbf{w}^H \mathrm{E}\left\{\mathbf{h}_1\mathbf{h}_1^H\right\}\mathbf{w} \quad (5)$$

$$P_{\mathbf{w}}^{\mathrm{I}} = \mathbf{w}^H \mathrm{E}\left\{\mathbf{H}_{\bar{1}}\mathbf{P}_{\bar{1}}\mathbf{H}_{\bar{1}}^H\right\}\mathbf{w} \quad (6)$$

$$P_{\mathbf{w}}^{\mathrm{N}} = \mathbf{w}^H\boldsymbol{\Sigma}\mathbf{w} + \sigma_n^2 \quad (7)$$

where $\mathbf{P}_{\bar{1}} \triangleq \mathrm{diag}\{p_2 \dots p_M\}$ and $\boldsymbol{\Sigma} \triangleq \sigma_v^2\mathrm{diag}\{|[\mathbf{f}]_1|^2 \dots |[\mathbf{f}]_k|^2\}$. Note that the expectations in (5)-(7) are taken with respect to the rays' directions θ_ls and their complex amplitude α_ls. Several approaches can be adopted to properly select the beamforming weights such as maximizing the received signal-to-interference-plus-noise ratio (SINR) subject to two different types of power constraints, namely the total transmit power constraint [7] and individual terminal power constraint [14], minimizing the total transmit power subject to the received quality of service constraint, or minimizing the interferences and noise power while maintaining the desired power equal to unity. In this paper, we are only concerned with the latter approach commonly known as MVDR CB. Let $\mathbf{w}_{\mathrm{mv}}$ denote its beamforming vector that satisfies

$$\mathbf{w}_{\mathrm{mv}} = \arg\min\left\{P^{\mathrm{I}} + P^{\mathrm{N}}\right\} \text{ s.t. } \mathbf{w}^H\mathrm{E}\left\{\mathbf{h}_1\mathbf{h}_1^H\right\}\mathbf{w} = 1. \quad (8)$$

The optimization problem in (8) can be rewritten as

$$\mathbf{w}_{\mathrm{mv}} = \arg\max \frac{\mathbf{w}^H\mathrm{E}\left\{\mathbf{h}_1\mathbf{h}_1^H\right\}\mathbf{w}}{\mathbf{w}^H\left(\mathrm{E}\left\{\mathbf{H}_{\bar{1}}\mathbf{P}_{\bar{1}}\mathbf{H}_{\bar{1}}^H\right\} + \boldsymbol{\Sigma}\right)\mathbf{w}} \quad \text{s.t.} \quad \mathbf{w}^H\mathrm{E}\left\{\mathbf{h}_1\mathbf{h}_1^H\right\}\mathbf{w} = 1. \quad (9)$$

Note that the derivation of $\mathbf{w}_{\mathrm{mv}}$ in closed form is a tedious task. Therefore, for the sake of analytical tractability, we expoit useful approximations of $\mathrm{E}\left\{\mathbf{h}_1\mathbf{h}_1^H\right\}$ and $\mathrm{E}\left\{\mathbf{H}_{\bar{1}}\mathbf{P}_{\bar{1}}\mathbf{H}_{\bar{1}}^H\right\}$. Using the fact that, for small values of σ_θ, the m-th transmitter can be seen as two non-scattered transmitters, the following approximation holds [9]-[13]:

$$\mathrm{E}\left\{\mathbf{h}_m\mathbf{h}_m^H\right\} \approx \frac{1}{2}\Big(\mathbf{a}\left(\phi_m+\sigma_\theta\right)\mathbf{a}\left(\phi_m+\sigma_\theta\right)^H + \mathbf{a}\left(\phi_m-\sigma_\theta\right)\mathbf{a}\left(\phi_m-\sigma_\theta\right)^H\Big) \quad (10)$$

where $\mathbf{a}(\phi) \triangleq \left[[\mathbf{a}(\phi)]_1 \dots [\mathbf{a}(\phi)]_K\right]^T$ with $[\mathbf{a}(\phi)]_k = [\mathbf{f}]_k e^{-j\frac{2\pi}{\lambda}r_k\cos(\phi-\psi_k)}$. It is noteworthy that the approximation in (10), previously exploited differently in angular spread and direction of arrival estimation of scattered sources [11], [12], is independent of the pdf $p(\theta)$. From (10), it follows that

$$\mathrm{E}\left\{\mathbf{H}_{\bar{1}}\mathbf{P}_{\bar{1}}\mathbf{H}_{\bar{1}}^H\right\} \approx \boldsymbol{\Gamma}\boldsymbol{\Lambda}\boldsymbol{\Gamma}^H \quad (11)$$

where $\boldsymbol{\Gamma} = \left[\mathbf{a}(\phi_2+\sigma_\theta), \mathbf{a}(\phi_2-\sigma_\theta), \dots, \mathbf{a}(\phi_M+\sigma_\theta), \mathbf{a}(\phi_M-\sigma_\theta)\right]$ and $\boldsymbol{\Lambda} = (1/2)\mathbf{P}_{\bar{1}}$. Therefore, (9) can be expressed as

$$\mathbf{w}_{\mathrm{mv}} = \arg\max \frac{\mathbf{w}^H\boldsymbol{\Xi}\mathbf{w}}{\mathbf{w}^H\left(\boldsymbol{\Gamma}\boldsymbol{\Lambda}\boldsymbol{\Gamma}^H + \boldsymbol{\Sigma}\right)\mathbf{w}} \quad \text{s.t.} \quad \mathbf{w}^H\boldsymbol{\Xi}\mathbf{w} = 2 \quad (12)$$

where $\boldsymbol{\Xi} = \mathbf{a}(\sigma_\theta)\mathbf{a}(\sigma_\theta)^H + \mathbf{a}(-\sigma_\theta)\mathbf{a}(-\sigma_\theta)^H$, or equivalently as,

$$\boldsymbol{\gamma}_{\mathrm{opt}} = \arg\max \frac{\boldsymbol{\gamma}^H\mathbf{A}^{-\frac{1}{2}}\boldsymbol{\Xi}\mathbf{A}^{-\frac{1}{2}}\boldsymbol{\gamma}}{\boldsymbol{\gamma}^H\boldsymbol{\gamma}} \quad \text{s.t.} \quad \boldsymbol{\gamma}^H\mathbf{A}^{-\frac{1}{2}}\boldsymbol{\Xi}\mathbf{A}^{-\frac{1}{2}}\boldsymbol{\gamma} = 2 \quad (13)$$

where $\boldsymbol{\gamma} = \mathbf{A}^{\frac{1}{2}}\mathbf{w}$ and $\mathbf{A} = \boldsymbol{\Gamma}\boldsymbol{\Lambda}\boldsymbol{\Gamma}^H + \boldsymbol{\Sigma}$. It is direct to show from (13) that $\boldsymbol{\gamma}_{\mathrm{opt}}$ is the principal eigenvector of the matrix $\mathbf{A}^{-\frac{1}{2}}\boldsymbol{\Xi}\mathbf{A}^{-\frac{1}{2}}$ scaled to satisfy the constraint in (13). Since $\mathbf{A}^{-\frac{1}{2}}$ is a full-rank matrix, the rank of $\mathbf{A}^{-\frac{1}{2}}\boldsymbol{\Xi}\mathbf{A}^{-\frac{1}{2}}$ is the same as the rank of $\boldsymbol{\Xi}$ that is inferior or equal to two. Therefore, $\mathbf{A}^{-\frac{1}{2}}\boldsymbol{\Xi}\mathbf{A}^{-\frac{1}{2}}$ has at most two eigenvectors. Moreover, it is straightforward to prove that, when σ_θ is relatively small, $\mathbf{A}^{-\frac{1}{2}}\left(\mathbf{a}(\sigma_\theta)+\mathbf{a}(-\sigma_\theta)\right)$ and $\mathbf{A}^{-\frac{1}{2}}\left(\mathbf{a}(\sigma_\theta)-\mathbf{a}(-\sigma_\theta)\right)$ are both eigenvectors of $\mathbf{A}^{-\frac{1}{2}}\boldsymbol{\Xi}\mathbf{A}^{-\frac{1}{2}}$ and, further, $\boldsymbol{\gamma}_{\mathrm{opt}} \approx \mu\mathbf{A}^{-\frac{1}{2}}\left(\mathbf{a}(\sigma_\theta)+\mathbf{a}(-\sigma_\theta)\right)$ [13]. Note that μ is the factor chosen such that the constraint in (13) is satisfied. Therefore, using the matrix inversion lemma, $\mathbf{w}_{\mathrm{mv}}$ is finally given by

$$\mathbf{w}_{\mathrm{mv}} = \mu\left(\boldsymbol{\Sigma}^{-1}\left(\mathbf{a}\left(\sigma_\theta\right)+\mathbf{a}\left(-\sigma_\theta\right)\right) - \boldsymbol{\Sigma}^{-1}\boldsymbol{\Gamma}\mathbf{d}\right) \quad (14)$$

where μ also satisfies the constraint in (12) and is given by

$$\mu = \left(\left\|\mathbf{A}^{-\frac{1}{2}}\left(\mathbf{a}\left(\sigma_\theta\right)+\mathbf{a}\left(-\sigma_\theta\right)\right)\right\|\left\|\mathbf{A}^{-\frac{1}{2}}\mathbf{a}\left(\sigma_\theta\right)\right\|\right)^{-1} \quad (15)$$

and

$$\mathbf{d} = \left(\boldsymbol{\Lambda}^{-1}+\boldsymbol{\Gamma}^H\boldsymbol{\Sigma}^{-1}\boldsymbol{\Gamma}\right)^{-1}\boldsymbol{\Gamma}^H\boldsymbol{\Sigma}^{-1}\left(\mathbf{a}\left(\sigma_\theta\right)+\mathbf{a}\left(-\sigma_\theta\right)\right). \quad (16)$$

Note that $\mathbf{w}_{\mathrm{mv}}$ is valid for any given pdf $p(\theta)$. Nevertheless, the MVDR CB is implementable in the wireless network of our concern only if the k-th terminal is able to compute its corresponding beamforming weight

$$[\mathbf{w}_{\mathrm{mv}}]_k = \mu\Bigg([\boldsymbol{\Sigma}]_{kk}^{-1}\left([\mathbf{a}\left(\sigma_\theta\right)]_k + [\mathbf{a}\left(-\sigma_\theta\right)]_k\right) - [\boldsymbol{\Sigma}]_{kk}^{-1}\sum_{m=1}^{2M-2}[\boldsymbol{\Gamma}]_{km}[\mathbf{d}]_m\Bigg). \quad (17)$$

According to A4, $[\boldsymbol{\Sigma}]_{kk}$, $[\mathbf{a}\left(\pm\sigma_\theta\right)]_k$ and the k-th row of $\boldsymbol{\Gamma}$ depend on the information commonly available at all terminals and, hence, are locally computable at the k-th terminal. However, it turns out that μ and the entries of $\mathbf{d}$ are functions of all terminals' locations and their forward channels. Unfortunately, the k-th terminal is oblivious to these information. Thus, terminals need to exchange their local information with one another. Let us denote by X the bandwidth allocated to share any given real between all terminals in the network. Since the k-th terminal must share its own coordinates (r_k, ψ_k) and its forward channel $[\mathbf{f}]_k$, the overall required bandwidth for the MVDR CB implementation is $3KX$. This amount linearly increases with K and becomes prohibitive in some applications such as wireless sensor networks (WSN) wherein the number of terminals (or sensor nodes) is typically large. Therefore, in such a case, the system's spectrum efficiency is significantly

reduced. Motivated by overcoming the aforementioned impediment, we present in the next session a novel DCB whose implementation does not require any bandwidth allocation, thereby improving the system's spectrum efficiency.

IV. Proposed DCB

When the beamforming response in the desired direction is fixed as for the MVDR CB presented in Section III, it has been shown that the transmit power from each terminal is inversely proportional to K while the SINR linearly increases with K [1], [13]. As such, using a large number of terminals results in both a substantial improvement in the signal reception quality and a considerable increase in the terminals' lifetime. As discussed above, this is at the cost of reducing the spectrum efficiency. In what follows, we will see how we can take advantage of large K without any loss of spectrum efficiency. Assuming that K is large enough, $\mathbf{d}$ and μ can be substituted with $\mathbf{d}^{\dagger} \triangleq \lim_{K\to\infty} \mathbf{d}$ and $\mu^{\dagger} \triangleq \lim_{K\to\infty} \mu$, respectively. Although being good approximations of $\mathbf{d}$ and μ for a large K, $\mathbf{d}^{\dagger}$ and $\mu^{\dagger}$ cannot be used in lieu of $\mathbf{d}$ and μ unless they depend solely on the information commonly available at all terminals. If the latter requirement is satisfied, the beamformer implementation does not require any bandwidth allocation and, hence, the system's spectrum efficiency is improved. The following lines prove that $\mathbf{d}^{\dagger}$ and $\mu^{\dagger}$ in fact satisfy this requirement. As $\lim_{K\to\infty} 1/(2Kp_m) = 0$, it can be shown that

$$\mathbf{d}^{\dagger} = \left(\lim_{K\to\infty} \frac{1}{K}\mathbf{\Gamma}^H\mathbf{\Sigma}^{-1}\mathbf{\Gamma}\right)^{-1} \times \left(\lim_{K\to\infty} \frac{1}{K}\mathbf{\Gamma}^H\mathbf{\Sigma}^{-1}\left(\mathbf{a}\left(\sigma_\theta\right)+\mathbf{a}\left(-\sigma_\theta\right)\right)\right). \quad (18)$$

First, let us derive the limit of the first expression in the righthand side (RHS) of (18). It follows from the definitions of $\mathbf{\Gamma}$ and $\mathbf{\Sigma}$ that

$$[\mathbf{\Gamma}^H\mathbf{\Sigma}^{-1}\mathbf{\Gamma}]_{mn} \triangleq \sum_{k=1}^{K} \frac{1}{\sigma_v^2} \times \begin{cases} e^{j\alpha\left(\phi_{\frac{n}{2}+1}-\phi_{\frac{m}{2}+1}\right)z_k^{(1)}} & m,n \text{ even} \\ e^{j\alpha\left(\phi_{\frac{n+3}{2}}-\phi_{\frac{m+3}{2}}\right)z_k^{(2)}} & m,n \text{ odd} \\ e^{j\alpha\left(\phi_{\frac{n+3}{2}}-\phi_{\frac{m}{2}+1}+2\sigma_\theta\right)z_k^{(3)}} & m \text{ even, } n \text{ odd} \\ e^{j\alpha\left(\phi_{\frac{n}{2}+1}-\phi_{\frac{m+3}{2}}-2\sigma_\theta\right)z_k^{(4)}} & m \text{ odd, } n \text{ even} \\ 1 & m=n \end{cases} \quad (19)$$

where $\alpha(\phi) \triangleq 4\pi R\sin(\phi/2)/\lambda$ and $z_k^{(i=1,\ldots,4)}$ for $k = 1,\ldots,K$ are i.i.d compound random variables with the following pdf:

$$f_{z_k^{(i=1,\ldots,4)}}(z) = \frac{2}{\pi}\sqrt{1-z^2}, \quad -1 \le z \le 1. \quad (20)$$

Using the strong law of large numbers and the fact that

$$\frac{2}{\pi}\int_{-1}^{1} e^{j\alpha(\phi)z}\sqrt{1-z^2}dz = 2\frac{J_1\left(\alpha\left(\phi\right)\right)}{\alpha\left(\phi\right)}, \quad (21)$$

we obtain the following result:

$$\lim_{K\to\infty} \frac{1}{K}[\mathbf{\Gamma}^H\mathbf{\Sigma}^{-1}\mathbf{\Gamma}] \xrightarrow{p1} \frac{2}{\sigma_v^2}\mathbf{E} \quad (22)$$

where $\mathbf{E}$ is a $(2M-2)\times(2M-2)$ matrix with

$$[\mathbf{E}]_{mn} \triangleq \begin{cases} \frac{J_1\left(\alpha\left(\phi_{\frac{n}{2}+1}-\phi_{\frac{m}{2}+1}\right)\right)}{\alpha\left(\phi_{\frac{n}{2}+1}-\phi_{\frac{m}{2}+1}\right)} & m,n \text{ even} \\ \frac{J_1\left(\alpha\left(\phi_{\frac{n+3}{2}}-\phi_{\frac{m+3}{2}}\right)\right)}{\alpha\left(\phi_{\frac{n+3}{2}}-\phi_{\frac{m+3}{2}}\right)} & m,n \text{ odd} \\ \frac{J_1\left(\alpha\left(\phi_{\frac{n+3}{2}}-\phi_{\frac{m}{2}+1}+2\sigma_\theta\right)\right)}{\alpha\left(\phi_{\frac{n+3}{2}}-\phi_{\frac{m}{2}+1}+2\sigma_\theta\right)} & m \text{ even, } n \text{ odd} \\ \frac{J_1\left(\alpha\left(\phi_{\frac{n}{2}+1}-\phi_{\frac{m+3}{2}}-2\sigma_\theta\right)\right)}{\alpha\left(\phi_{\frac{n}{2}+1}-\phi_{\frac{m+3}{2}}-2\sigma_\theta\right)} & m \text{ odd, } n \text{ even} \\ \frac{1}{2} & m=n \end{cases} \quad (23)$$

Using the strong law of large numbers, it can be also shown that

$$\lim_{K\to\infty} \frac{1}{K}\mathbf{\Gamma}^H\mathbf{\Sigma}^{-1}\left(\mathbf{a}\left(\sigma_\theta\right)+\mathbf{a}\left(-\sigma_\theta\right)\right) \xrightarrow{p1} \frac{2}{\sigma_v^2}\mathbf{z} \quad (24)$$

where $\mathbf{z}$ is a $(2M-2)\times 1$ vector with

$$[\mathbf{z}]_m \triangleq \begin{cases} \frac{J_1\left(\alpha\left(\phi_{\frac{m}{2}+1}-2\sigma_\theta\right)\right)}{\alpha\left(\phi_{\frac{m}{2}+1}-2\sigma_\theta\right)} + \frac{J_1\left(\alpha\left(\phi_{\frac{m}{2}+1}\right)\right)}{\alpha\left(\phi_{\frac{m}{2}+1}\right)} & m \text{ even} \\ \frac{J_1\left(\alpha\left(\phi_{\phi_{\frac{m+3}{2}}}+2\sigma_\theta\right)\right)}{\alpha\left(\phi_{\phi_{\frac{m+3}{2}}}+2\sigma_\theta\right)} + \frac{J_1\left(\alpha\left(\phi_{\phi_{\frac{m+3}{2}}}\right)\right)}{\alpha\left(\phi_{\phi_{\frac{m+3}{2}}}\right)} & m \text{ odd} \end{cases}. \quad (25)$$

Therefore, it follows from (22) and (24) that

$$\mathbf{d}^{\dagger} \xrightarrow{ep1} \mathbf{E}^{-1}\mathbf{z}. \quad (26)$$

Equations (23) and (25) show that $\mathbf{E}$ and $\mathbf{z}$ depend only on the information commonly available at all terminals and, hence, all the entries of $\mathbf{d}^{\dagger}$ can be locally computed at each terminal. Following a similar approach as above, it can be readily proven that

$$\mu^{\dagger} \xrightarrow{p1} \left(\frac{\sigma_v^4}{2K^2\left(1+2\frac{J_1(\alpha(2\sigma_\theta))}{\alpha(2\sigma_\theta)} - \mathbf{z}^T\mathbf{d}^{\dagger}\right)}\right)^{\frac{1}{2}}. \quad (27)$$

It can be observed from (27) that $\mu^{\dagger}$ does not depend on the location and the forward channel of any terminal and, therefore, it is locally computable at each terminal. Substituting $\mathbf{d}$ and μ by their respective counterparts $\mathbf{d}^{\dagger}$ and $\mu^{\dagger}$, we introduce a new DCB whose beamforming vector is

$$\mathbf{w}_{\sigma_\theta}^{\dagger} = \mu^{\dagger}\left(\mathbf{\Sigma}^{-1}\left(\mathbf{a}\left(\sigma_\theta\right)+\mathbf{a}\left(-\sigma_\theta\right)\right) - \mathbf{\Sigma}^{-1}\mathbf{\Gamma}\mathbf{d}^{\dagger}\right). \quad (28)$$

Note that $\mathbf{w}_{\sigma_\theta}^{\dagger}$ well-approximates $\mathbf{w}_{\text{mv}}$ for a large K and, further, its implementation does not require any bandwidth allocation, thereby improving the system's spectrum efficiency. Moreover, the proposed DCB takes into account the presence of local scattering in the transmitters' vicinities

and its beamforming vector $\mathbf{w}_{\sigma_\theta}^{\dagger}$ is valid for any given pdf $p(\theta)$. It is also noteworthy that $\mathbf{w}_0^{\dagger}$ is the beamforming vector associated with the scattering-free DCB, which is designed without taking into account the presence of local scattering in the transmitters's vicinities. According to (28), $\mathbf{w}_0^{\dagger}$ is in agreement with the results in [7], [8] where interferences are considered and the local scattering phenomenon is neglected.

V. Proposed DCB vs scattering-free DCB

One way to prove the efficiency of the proposed DCB technique is undoubtedly comparing its achieved SINR with the SINR achieved when the scattering-free DCB technique, which is designed without taking into account the presence of local scattering in the transmitters's vicinities, is used in the wireless network. To this end, we introduce the following performance measure:

$$\Upsilon\left(\sigma_\theta\right) = \frac{\xi_{\mathbf{w}_0^{\dagger}}}{\xi_{\mathbf{w}_{\sigma_\theta}^{\dagger}}}, \tag{29}$$

where

$$\xi_{\mathbf{w}} = \frac{P_{\mathbf{w}}(\phi_1)}{\sum_{m=2}^{M} P_{\mathbf{w}}(\phi_m) + P_{\mathbf{w}}^{\mathrm{N}}}, \tag{30}$$

is the achieved SINR when the beamforming vector $\mathbf{w}$ is used in the wireless network. In (30), commonly known as the beampattern, $P_{\mathbf{w}}(\phi_\star) = p_\star \left\| \mathbf{w}^H \sum_{l=1}^{L} \alpha_l \mathbf{a}(\phi_\star + \theta_l) \right\|^2$ is the received power from a transmitter at direction $\phi_\star$ with power $p_\star$. It can be easily seen that $\Upsilon\left(\sigma_\theta\right)$ is an excessively complex function of the random variables r_k, ψ_k, $[\mathbf{f}]_k$ for $k = 1, \ldots, K$ and α_l, θ_l for $l = 1, \ldots, L$ and, hence, a random quantity of its own. Therefore, it is practically more appealing to investigate the behavior and the properties of $\tilde{\Upsilon}\left(\sigma_\theta\right)$ given by

$$\tilde{\Upsilon}\left(\sigma_\theta\right) = \frac{\tilde{\xi}_{\mathbf{w}_0^{\dagger}}}{\tilde{\xi}_{\mathbf{w}_{\sigma_\theta}^{\dagger}}}, \tag{31}$$

where $\tilde{\xi}_{\mathbf{w}} = \tilde{P}_{\mathbf{w}}(\phi_1) / \left(\sum_{m=2}^{M} \tilde{P}_{\mathbf{w}}(\phi_m) + \tilde{P}_{\mathbf{w}}^{\mathrm{N}} \right)$ is the achieved average-signal-to-average-interference-plus-noise ratio (ASAINR) when $\mathbf{w}$ is implemented in the WSN with $\tilde{P}_{\mathbf{w}}(\phi_\star) = \mathrm{E}\left\{P_{\mathbf{w}}(\phi_\star)\right\}$, called the average beampattern, and $\tilde{P}_{\mathbf{w}}^{\mathrm{N}} = \mathrm{E}\left\{P_{\mathbf{w}}^{\mathrm{N}}\right\}$. Thus, using the proposed DCB technique, it can be shown that

$$\tilde{P}_{\mathbf{w}_{\sigma_\theta}^{\dagger}}^{\mathrm{N}} = \frac{\sigma_v^2}{K} + {\sigma_n}^2, \tag{32}$$

and

$$\tilde{P}_{\mathbf{w}_{\sigma_\theta}^{\dagger}}\left(\phi_\star\right) = \frac{p_\star}{K} \left(1 + \frac{2(K-1)\Omega\left(\phi_\star\right)}{\left(1 + 2\frac{J_1(\alpha(2\sigma_\theta))}{\alpha(2\sigma_\theta)} - \mathbf{z}^T \mathbf{d}^{\dagger} \right)} \right), \tag{33}$$

where

$$\Omega\left(\phi_\star\right) = \int p(\theta) \left(\frac{J_1\left(\alpha\left(\phi_\star + \theta + \sigma_\theta\right)\right)}{\alpha\left(\phi_\star + \theta + \sigma_\theta\right)} + \frac{J_1\left(\alpha\left(\phi_\star + \theta - \sigma_\theta\right)\right)}{\alpha\left(\phi_\star + \theta - \sigma_\theta\right)} - \mathbf{z}_{\phi_\star + \theta}^T \mathbf{d}^{\dagger} \right)^2 d\theta. \tag{34}$$

In (34), $\mathbf{z}_{\phi+\theta}$ is a $(2M-2) \times 1$ vector such that

$$[\mathbf{z}_{\phi+\theta}]_m \triangleq \begin{cases} \dfrac{J_1\left(\alpha\left(\phi - \phi_{\frac{m}{2}+1} + \theta + \sigma_\theta\right)\right)}{\alpha\left(\phi - \phi_{\frac{m}{2}+1} + \theta + \sigma_\theta\right)} & m \text{ even} \\ \dfrac{J_1\left(\alpha\left(\phi - \phi_{\frac{m+3}{2}} + \theta - \sigma_\theta\right)\right)}{\alpha\left(\phi - \phi_{\frac{m+3}{2}} + \theta - \sigma_\theta\right)} & m \text{ odd} \end{cases}. \tag{35}$$

In turn, when the scattering-free DCB technique is implemented in the wireless network, it can be proved that

$$\tilde{P}_{\mathbf{w}_0^{\dagger}}^{\mathrm{N}} = \frac{\sigma_v^2}{K} + {\sigma_n}^2, \tag{36}$$

and

$$\tilde{P}_{\mathbf{w}_0^{\dagger}}\left(\phi_\star\right) = \frac{p_\star}{K} \left(1 + \frac{4(K-1)\Delta\left(\phi_\star\right)}{1 - 2\boldsymbol{\upsilon}_0^T \mathbf{c}} \right), \tag{37}$$

where

$$\Delta\left(\phi_\star\right) = \int p(\theta) \left(\frac{J_1(\alpha(\phi_\star + \theta))}{\alpha(\phi_\star + \theta)} - \boldsymbol{\upsilon}_{\phi_\star + \theta}^T \mathbf{c} \right)^2 d\theta. \tag{38}$$

In (37) and (38), $\boldsymbol{\upsilon}_\phi$ and $\mathbf{c}$ are $(M-1) \times 1$ vectors defined in [7]. It is noteworthy that the integrals in (34) and (38) can be computed numerically with any desired accuracy by using the most popular mathematical software packages such as Matlab and Mathematica, after properly choosing the pdf $p(\theta)$. In fact, several statistical distributions for θ_l have been proposed, so far, such as Laplacian, Gaussian or uniform [10]-[13]. Using (32)-(38), simulations in Section VI prove that the proposed DCB technique is much more efficient in terms of achieved ASAINR compared to the scattering-free DCB, which is designed without taking into account the presence of local scattering. This result holds for any given pdf $p(\theta)$. Moreover, it can be shown that

$$\lim_{K \to \infty} \tilde{\Upsilon}\left(\sigma_\theta\right) = \lim_{K \to \infty} \bar{\Upsilon}\left(\sigma_\theta\right), \tag{39}$$

where $\bar{\Upsilon}\left(\sigma_\theta\right) = \bar{\xi}_{\mathbf{w}_0^{\dagger}} / \bar{\xi}_{\mathbf{w}_{\sigma_\theta}^{\dagger}}$ with $\bar{\xi}_{\mathbf{w}} = \mathrm{E}\left\{\xi_{\mathbf{w}}\right\}$ is the average SINR (ASINR) which is a more practical performance measure but analytically intractable. Therefore, $\tilde{\Upsilon}\left(\sigma_\theta\right)$ is a meaningful performance measure whose behavior approaches that of $\bar{\Upsilon}\left(\sigma_\theta\right)$ when K is large enough. This proves that, for large K, the proposed DCB technique is also much more robust against local scattering than its scattering-free vis-a-vis in terms of achieved ASINR.

VI. Simulation Results

All the simulation results are obtained by averaging over 10^6 random realizations of r_k, ψ_k, $[\mathbf{f}]_k$ for $k = 1, \ldots, K$ and α_l, θ_l for $l = 1, \ldots, L$. In all examples, we assume that all transmitters have the same power p, the noises' powers σ_n^2 and σ_v^2 are 10-dB below p, $R = 1$ and $K = 20$. It is also assumed that the number of rays is $L = 6$ and that their phases are uniformly distributed. Fig. 2 plots $\tilde{\xi}_{\mathbf{w}_{\sigma_\theta}^{\dagger}}$ and $\tilde{\xi}_{\mathbf{w}_0^{\dagger}}$ versus σ_θ when $M = 3$. As can be observed from this figure, the simulated and the analytical ASAINRs $\tilde{\xi}_{\mathbf{w}}$ perfectly match for both $\mathbf{w} = \mathbf{w}_{\sigma_\theta}^{\dagger}$ and $\mathbf{w} = \mathbf{w}_0^{\dagger}$. In addition, the proposed DCB turns out to be much more

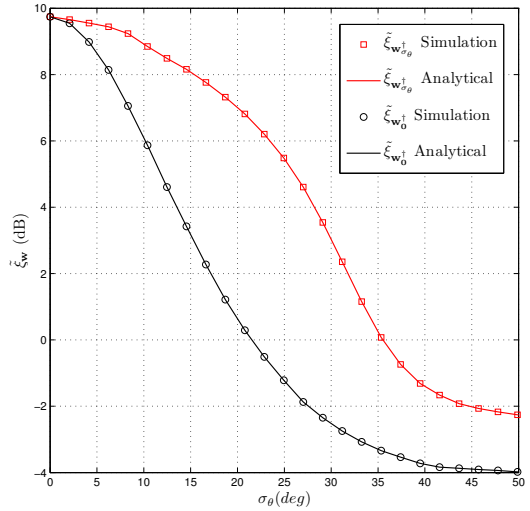

Fig. 2. $\tilde{\xi}_{\mathbf{w}^{\dagger}_{\sigma_\theta}}$ and $\tilde{\xi}_{\mathbf{w}^{\dagger}_{0}}$ versus σ_θ when $M = 3$.

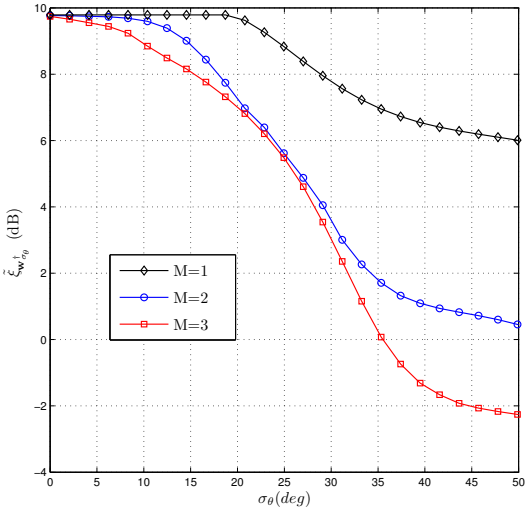

Fig. 3. $\tilde{\xi}_{\mathbf{w}^{\dagger}_{\sigma_\theta}}$ versus σ_θ for $M = 1$, $M = 2$ and $M = 3$.

robust against local scattering than its scattering-free DCB vis-a-vis, which is designed without taking into account the presence of local scattering in the source and interferences vicinities. In fact, as it can be verified from Fig. 2, the performance of the latter seems to be acceptable in rural environments, but becomes more and more unsatisfactory in the suburban and urban environments wherein local scattering is more important. In such environments, the proposed technique achieves until 6 dB of ASINR gain. Fig. 3 displays $\tilde{\xi}_{\mathbf{w}^{\dagger}_{\sigma_\theta}}$ for $M = 1$, $M = 2$ and $M = 3$. As can be seen in this figure, the sensitivity of the proposed DCB to the local scattering phenomenon increases with the number of interfering transmitters.

VII. Conclusion

In this paper, we considered the minimum variance distortionless response (MVDR) CB to achieve a dual-hop communication from a far-field source surrounded by several interfering transmitters to a receiver, through a wireless network comprised of K independent terminals. Each transmitter (source or interference) is assumed to be scattered by a large number of scatterers within its vicinity to generate L i.i.d rays from the transmit signal. Taking into account this phenomenon, the beamforming vector was derived. Unfortunately, it is shown that the MVDR CB implementation requires large bandwidth allocation, thereby decreasing the system's spectrum efficiency. An alternative DCB whose implementation does not require any bandwidth allocation and, further, that well-approximates its MVDR CB counterpart was then proposed. The performance of the proposed technique was analyzed and its advantages against the scattering-free DCB technique, which is designed without taking into account the presence of local scattering in the source and interferences vicinities, were verified. It was proved that the proposed technique is much more robust against local scattering than its so-called scattering-free vis-a-vis and, further, is able to achieve until 6 dB of ASAINR gain.

References

[1] H. Ochiai, P. Mitran, H. V. Poor, and V. Tarokh, "Collaborative beamforming for distributed wireless ad hoc sensor networks," *IEEE Trans. Signal Process.,* vol. 53, pp. 4110-4124, Nov. 2005.

[2] M. F. A. Ahmed and S. A. Vorobyov, "Collaborative beamforming for wireless sensor networks with Gaussian distributed sensor nodes," *IEEE Trans. Wireless Commun.,* vol. 8, pp. 638-643, Feb. 2009.

[3] K. Zarifi, S. Affes, and A. Ghrayeb, "Distributed beamforming for wireless sensor networks with improved graph connectivity and energy efficiency," *IEEE Trans. Signal Process.,* vol. 58, pp. 1904-1921, Mar. 2010.

[4] M. F. A. Ahmed and S. A. Vorobyov, "Sidelobe control in collaborative beamforming via node selection," *IEEE Trans. Signal Process.,* vol. 58, pp. 6168-6180, Dec. 2010.

[5] M. Pun, D. R. Brown III, and H. V. Poor, "Opportunistic collaborative beamforming with one-bit feedback," *IEEE Trans. Wireless Commun.,* vol. 8, pp. 2629-2641, May 2009.

[6] L. C. Godara, "Application of antenna arrays to mobile communications, Part II: Beam-forming and direction-of-arrival considerations," it Proc. IEEE, vol. 85, pp. 11951245, Aug. 1997

[7] K. Zarifi, S. Zaidi, S. Affes, and A. Ghrayeb, "A distributed amplify-and-forward beamforming technique in wireless sensor networks," *IEEE Trans. Signal Process.,* vol. 59, pp. 36573674, Aug. 2011.

[8] K. Zarifi, S. Affes, and A. Ghrayeb, "Collaborative null-steering beamforming for uniformly distrubuted wireless sensor networks," *IEEE Trans. Signal Process.,* vol. 58, pp. 1889-1903, Mar. 2010.

[9] D. Astly and B. Ottersten, "The effects of local scattering on direction of arrival estimation with MUSIC," *IEEE Trans. Signal Process.,* vol. 47, pp. 32203234, Dec. 1999.

[10] A. Amar, "The effect of local scattering on the gain and beamwidth of a collaborative beampattern for wireless sensor networks," *IEEE Trans. Wireless Commun.,* vol. 9, pp. 27302736, Sep. 2010.

[11] M. Souden, S. Affes, and J. Benesty, "A two-stage approach to estimate the angles of arrival and the angular spreads of locally scattered sources," *IEEE Trans. Signal Process.,* vol. 56, pp. 19681983, May 2008.

[12] M. Bengtsson and B. Ottersten, "Low-complexity estimators for distributed sources," *IEEE Trans. Signal Process.,* vol. 48, pp. 21852194, Aug. 2000.

[13] S. Zaidi and S. Affes, "Distributed collaborative beamforming with minimum overhead for local Scattering environments," *IEEE IWCMC,* Cyprus, Aug. 2012. Invited paper.

[14] V. Havary-Nassab, S. Shahbazpanahi, A. Grami, and Z.-Q. Luo, "Distributed beamforming for relay networks based on second-order statistics of the channel state information," *IEEE Trans. Signal Process.,* vol. 56, pp. 43064316, Sep. 2008.